

Seminar Recent Advances in Geometry Processing
Final presentation
February 27, 2025

SuGaR: Surface-Aligned Gaussian Splatting for Efficient 3D Mesh Reconstruction and High-Quality Mesh Rendering

Antoine Guédon and Vincent Lepetit. In *Proceedings of the IEEE/CVF Conference on Computer Vision and Pattern Recognition*, pages 5354–5363, 2024.

Presented by
Bertan Karacora
Institute of Computer Science, University of Bonn
bertan.karacora@uni-bonn.de

Contents

1. Introduction
2. Background
3. Methods
4. Results
5. Discussion
6. Conclusion

Contents

- 1. Introduction**
2. Background
3. Methods
4. Results
5. Discussion
6. Conclusion

Capturing real-world scenes

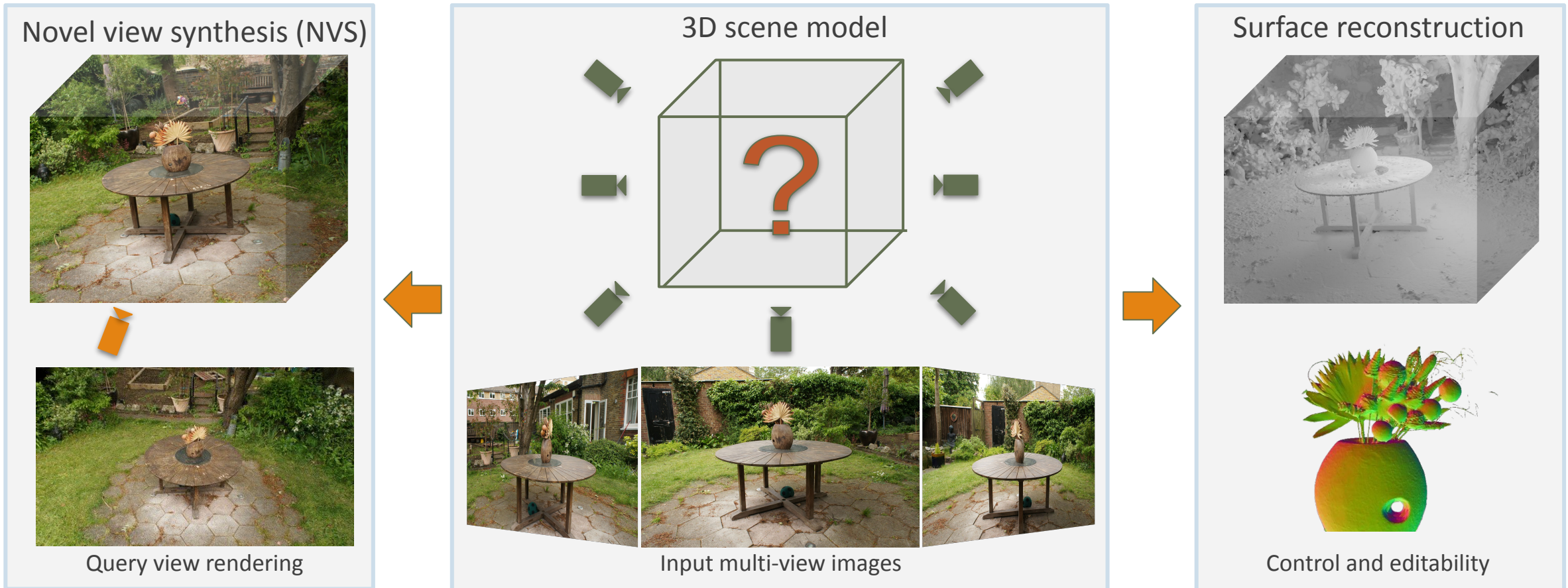


Figure 1: Concept of the problem of capturing real-world scenes from photographs. A virtual scene model is created from multi-view images. This model can be used for novel view synthesis, i.e., rendering an image of the scene from a query view-point. At the same time, surface reconstruction aims to provide 3D information that enables structural analysis and manipulation of the scene. Images adapted from [1, 2, 3].

➤ How to combine visual expressiveness and constrained geometry?

3D representations

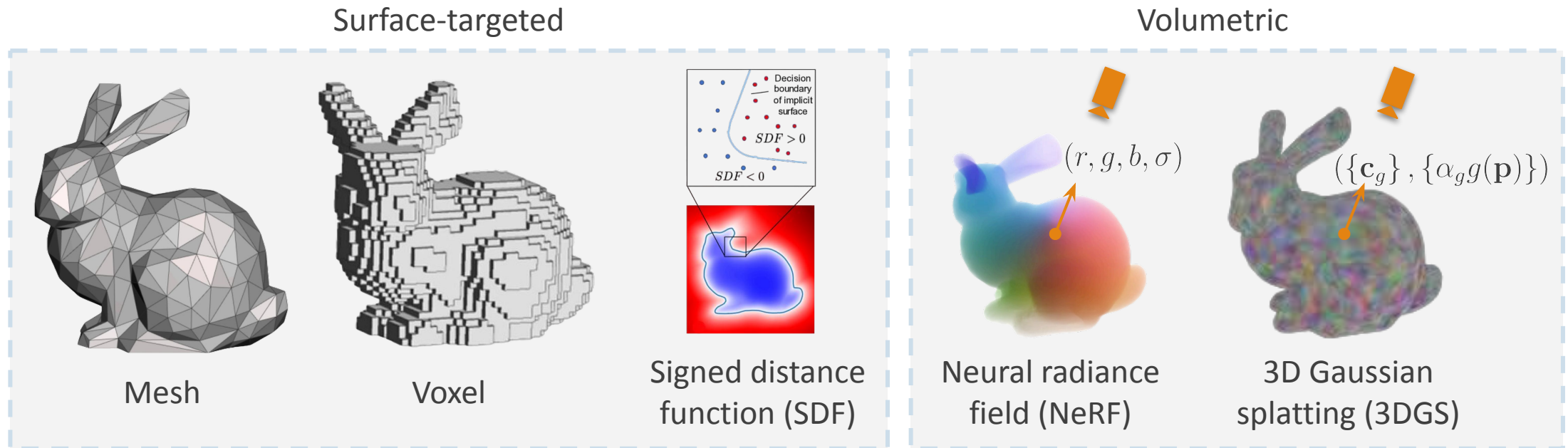


Figure 2: A selection of common 3D representations. Images adapted from [4, 5, 6, 7].

- Recent success of volumetric representations for NVS

- Great representation power

- Sidestep the global illumination problem

[4] Matt Tancik, Ben Mildenhall, Prav Srikanth, Ian Buck, and Antoni Balazs. Neural Volumetric Rendering for Computer Vision. ECCV 2022 Tutorial, 2022.

[5] Prasoon Kumar Vinodkumar, Dogus Karabulut, Egils Avots, Cagri Ozcinar, and Gholamreza Anbarjafari. Deep Learning for 3D Reconstruction, Augmentation, and Registration: A Review Paper. *Entropy*, 26(3):235, 2024.

[6] Jeong Joon Park, Peter Florence, Julian Straub, Richard Newcombe, and Steven Lovegrove. DeepSDF: Learning Continuous Signed Distance Functions for Shape Representation. In *Proceedings of the IEEE/CVF conference on computer vision and pattern recognition*, pages 165–174, 2019.

[7] Jan-Niklas Dihlmann, Arjun Majumdar, Andreas Engelsdorff, Raphael Braun, and Hendrik Leinisch. Subsurface Scattering for 3D Gaussian Splatting. *arXiv preprint arXiv:2408.12282*, 2024.

NeRFs for surface reconstruction

- Naive approach: Apply Marching Cubes [8] on volume density
- SOTA: Volume density as transformed SDF
 - Example: Neuralangelo [10]

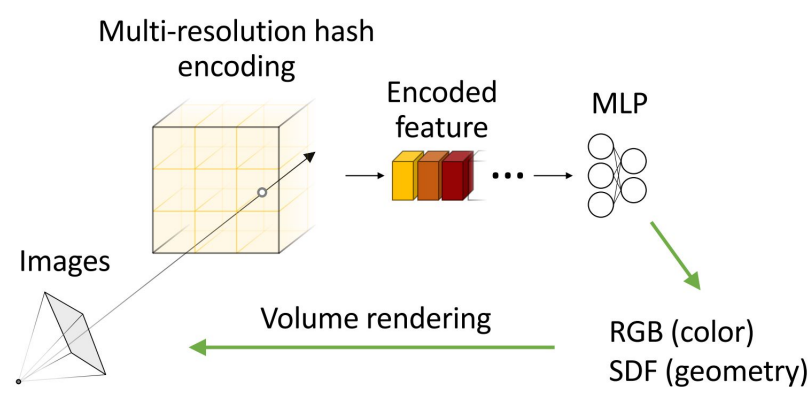


Figure 3: Pipeline of Neuralangelo. From [11].

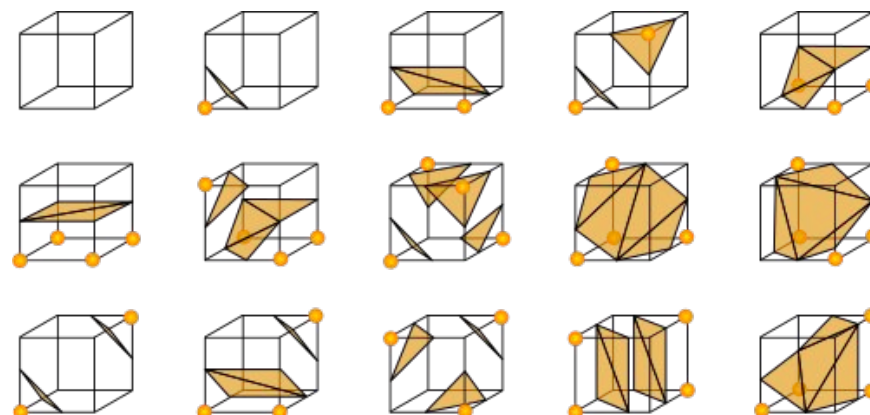


Figure 4: All possible polygon configurations in Marching Cubes when exploiting rotation and reflection symmetries. From [9].

[8] William E Lorensen and Harvey E Cline. Marching cubes: A high resolution 3D surface construction algorithm. In *Seminal graphics: pioneering efforts that shaped the field*, pages 347–353. 1998.

[9] Ryoshozu. The originally published 15 cube configurations. Wikimedia Commons. <https://commons.wikimedia.org/wiki/File:MarchingCubesEdit.svg>. Accessed: February 25, 2025.

[10] Zhaoshuo Li, Thomas Müller, Alex Evans, Russell H Taylor, Mathias Unberath, Ming-Yu Liu, and Chen-Hsuan Lin. Neuralangelo: High-Fidelity Neural Surface Reconstruction. In *Proceedings of the IEEE/CVF Conference on Computer Vision and Pattern Recognition*, pages 8456–8465, 2023.

[11] Zhaoshuo Li, Thomas Müller, Alex Evans, Russell H Taylor, Mathias Unberath, Ming-Yu Liu, and Chen-Hsuan Lin. Poster for Neuralangelo. <https://research.nvidia.com/labs/dir/neuralangelo/poster.pdf>. Accessed: February 25, 2025.

Surface reconstruction from 3DGs?

- Limited correspondence to the surface
 - Scene consists of Gaussian primitives with unconstrained positioning
 - No structure or topology
- Naive approach leads to disconnected surface
 - Naive density measure derived from the Gaussians is sparse

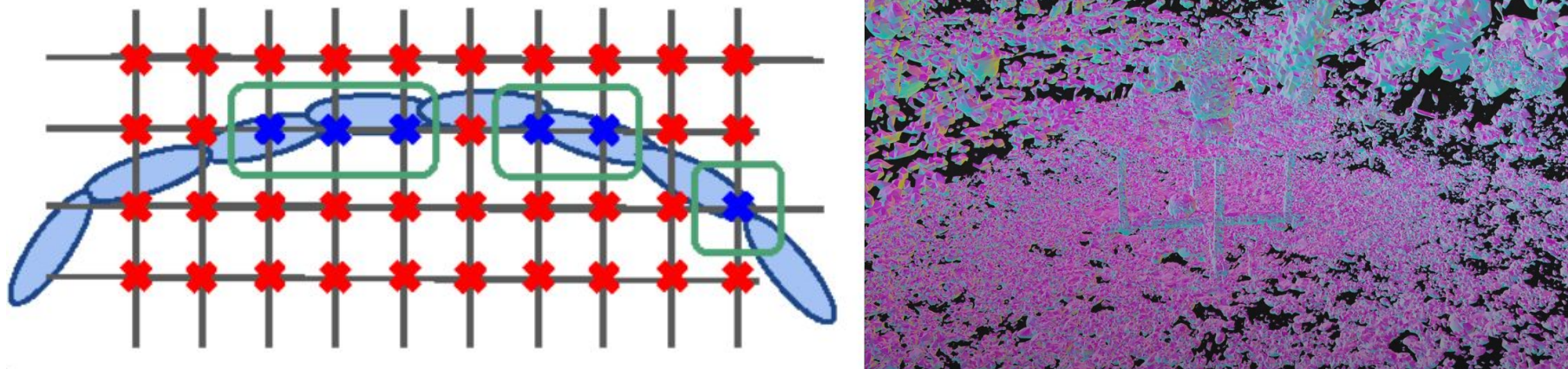


Figure 5: Left: Marching Cubes fails to reconstruct a connected surface due to the small extend of many Gaussians. With increasing voxel resolution, the required number of samples becomes excessive. Right: A reconstructed scene using the naive approach. Adapted from [12].

[12] Antoine Guédon and Vincent Lepetit. Poster for SuGaR. <https://cvpr.thecvf.com/media/PosterPDFs/CVPR%202024/30910.png>. Accessed: February 25, 2025.

Motivating SuGaR [1]

- Construct a high-quality mesh for a scene via 3DGS
 - Regularize Gaussians to be surface-aligned and well-distributed
 - Extract a surface mesh efficiently
 - Bind Gaussians to the mesh and jointly refine both
- Enable traditional mesh editing tools, physics-based simulations, etc.

[1] Antoine Guédon and Vincent Lepetit. In *Proceedings of the IEEE/CVF Conference on Computer Vision and Pattern Recognition*, pages 5354–5363, 2024.

Contents

1. Introduction
- 2. Background**
3. Methods
4. Results
5. Discussion
6. Conclusion

Volume rendering and radiance fields

Ray-sampling and alpha-blending:

$$C = \sum_i^N T_i \alpha_i \mathbf{c}_i \quad \text{with} \quad \alpha_i = 1 - \exp(-\sigma_i \delta_i), \quad T_i = \prod_{j=1}^{i-1} (1 - \alpha_j)$$

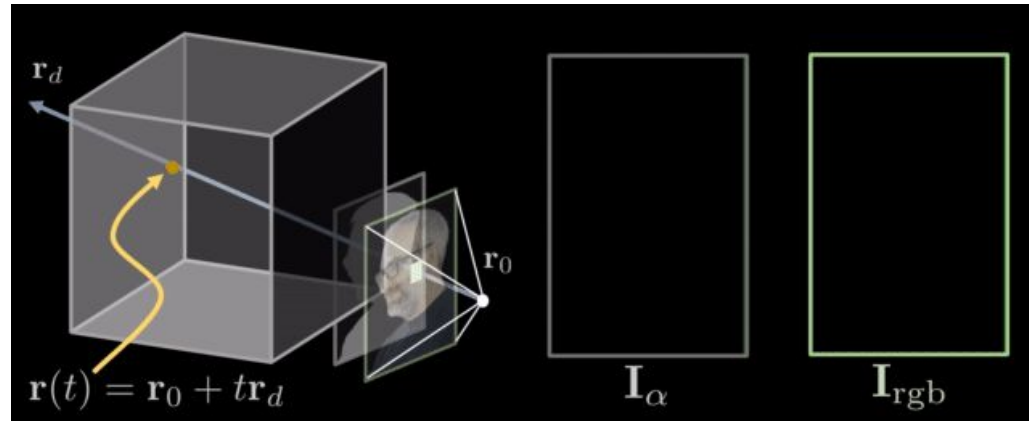


Figure 8: Visualization of differentiable ray marching. A line integral is computed through the volume along the ray defined by each pixel. From [16].

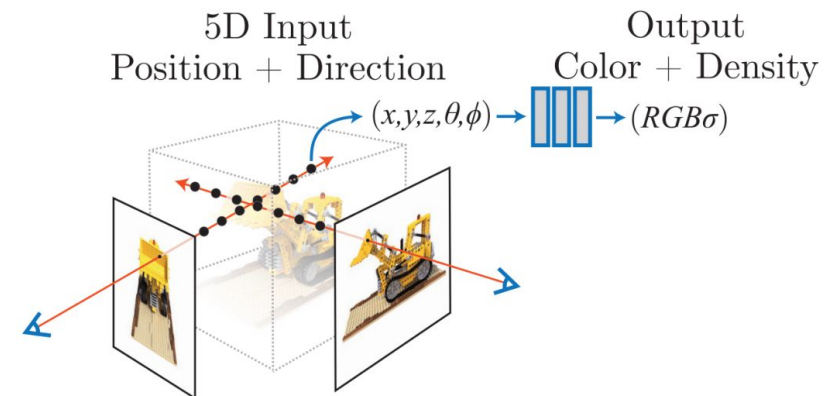


Figure 9: NeRF parameterizes a 3D scene as a 3D neural field mapping 3D coordinates to radiance and density. From [17].

[16] Stephen Lombardi. Neural Volumes. <https://stephenlombardi.github.io/projects/neuralvolumes>. Accessed: February 17, 2025.

[17] Yiheng Xie, Towaki Takikawa, Shunsuke Saito, Or Litany, Shiqin Yan, Numair Khan, Federico Tombari, James Tompkin, Vincent Sitzmann, and Srinath Sridhar. Neural Fields in Visual Computing and Beyond. In *Computer Graphics Forum*, pages 641–676. 2022.

3DGS scene model

- Scene primitives: 3D Gaussians $g(\mathbf{p}) = \exp\left(-\frac{1}{2}(\mathbf{p} - \mathbf{p}_g)^\top \Sigma_g^{-1}(\mathbf{p} - \mathbf{p}_g)\right)$
 - position $\mathbf{p}_g \in \mathbb{R}^3$
 - scaling vector $\mathbf{s}_g \in \mathbb{R}^3$
 - quaternion $\mathbf{q}_g \in \mathbb{R}^4$
 - opacity $\alpha_g \in [0, 1]$
 - spherical harmonics $\mathbf{c}_g \in \mathbb{R}^{(\ell+1)^2}$ up to degree ℓ

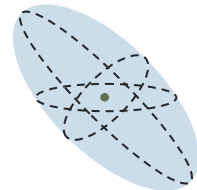


Figure 10: Visualization of a 3D Gaussian.

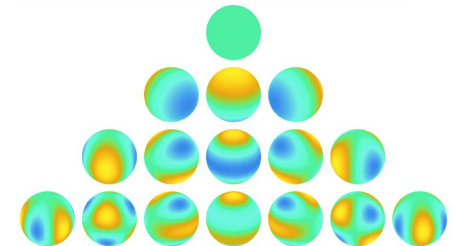


Figure 11: Real spherical harmonics up to degree 3. From [18]

[18] Florian Pfaff, Gerhard Kurz, and Uwe D Hanebeck. Filtering on the Unit Sphere Using Spherical Harmonics. In *2017 IEEE International Conference on Multisensor Fusion and Integration for Intelligent Systems (MFI)*, pages 124–130. 2017.

Splatting the Gaussians

- Volume rendering but no more sampling
- Projected covariance $\Sigma'_g = JW\Sigma_g W^\top J^\top$

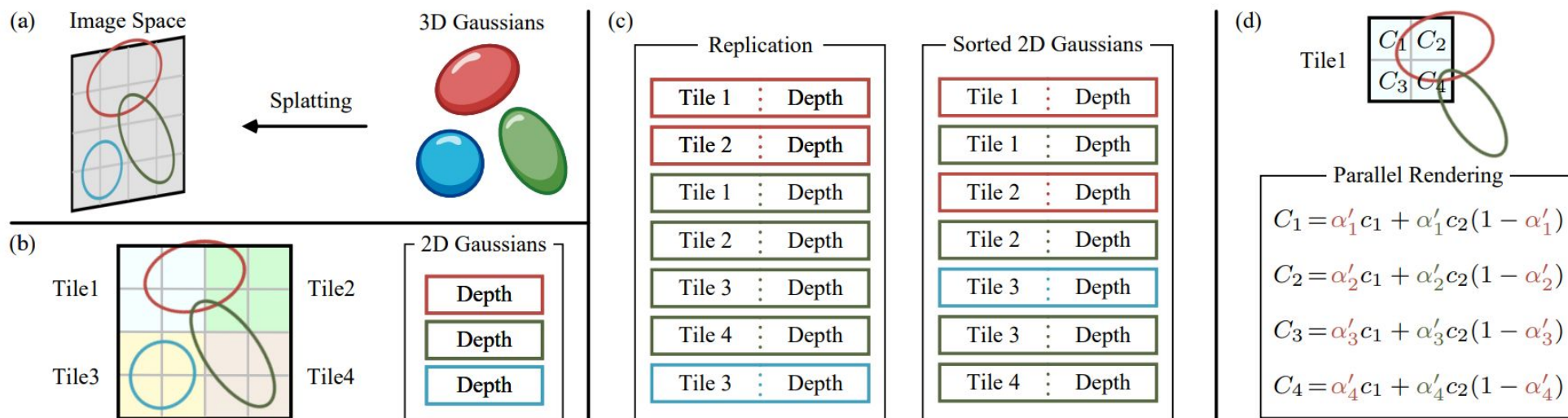


Figure 12: An illustration of the forward process of 3DGS. (a) The splatting step projects 3D Gaussians into image space. (b) 3DGS divides the image into multiple non-overlapping patches, i.e., tiles. (c) 3DGS replicates the Gaussians which cover several tiles, assigning each copy an identifier, i.e., a tile ID. (d) By rendering the sorted Gaussians, all pixels within the tile are obtained. The computational workflows for pixels and tiles are independent and can be done in parallel. From [19].

[19] Guikun Chen and Wenguan Wang. A Survey on 3d Gaussian Splatting. *arXiv preprint arXiv:2401.03890*, 2024.

Optimization

- Fast rasterization for efficiency during iterative optimization
- Objective: $L = (1 - \lambda)L_1 + \lambda L_{\text{D-SSIM}}$

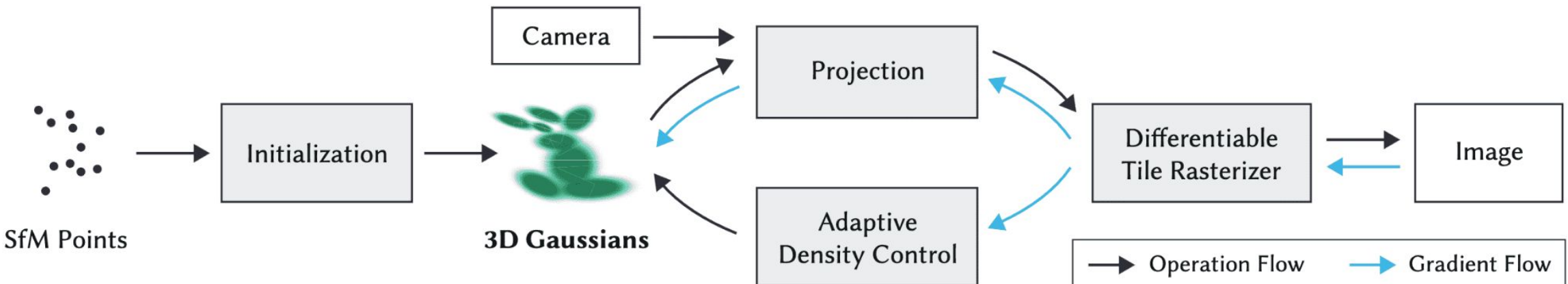


Figure 13: Optimization pipeline of 3DGs. A set of 3D Gaussians is initialized from a sparse SfM point cloud. Then, this set of Gaussians is optimized and adaptively controlled for density. During optimization, the fast tile-based renderer allows competitive training times compared to SOTA fast radiance field methods. From [20].

[20] Bernhard Kerbl, Georgios Kopanas, Thomas Leimkühler, and George Drettakis. 3D Gaussian Splatting for Real-time Radiance Field Rendering. *ACM Trans. Graph.*, 42(4):139-1, 2023.

Contents

1. Introduction
2. Background
- 3. Methods**
4. Results
5. Discussion
6. Conclusion

Overview

1. Initialize the scene using original 3DGS
2. Regularize Gaussians to be opaque using entropy term
3. Regularize Gaussians to correspond to the surface
4. Extract a mesh
5. Jointly refine Gaussians and mesh

Surface-alignment regularization

Approach: Assume goal is achieved to derive a SDF

- Density measure:

$$d(\mathbf{p}) = \sum_g \alpha_g g(\mathbf{p})$$

- Assume Gaussians have limited overlap:

$$d(\mathbf{p}) \approx \alpha_{g^*} g^*(\mathbf{p}) = \exp\left(-\frac{1}{2}(\mathbf{p} - \mathbf{p}_{g^*})^\top \Sigma_{g^*}^{-1}(\mathbf{p} - \mathbf{p}_{g^*})\right)$$

- Assume Gaussians are flat and surface-aligned:

$$\Sigma_{g^*} = V \text{diag}(s_1^2, s_2^2, s_3^2) V^\top \quad \text{with} \quad s_{g^*} = s_3 \ll s_1, s_2$$

$$(\mathbf{p} - \mathbf{p}_{g^*})^\top \Sigma_{g^*} (\mathbf{p} - \mathbf{p}_{g^*}) = \sum_{i=1}^3 \frac{1}{s_i^2} \langle \mathbf{p} - \mathbf{p}_{g^*}, v_i \rangle^2 \approx \frac{1}{s_{g^*}^2} \langle \mathbf{p} - \mathbf{p}_{g^*}, n_{g^*} \rangle^2$$

Surface-alignment regularization

- Assume Gaussians are opaque:

$$\bar{d}(\mathbf{p}) = \exp\left(-\frac{1}{2s_{g^*}^2}\langle \mathbf{p} - \mathbf{p}_{g^*}, \mathbf{n}_{g^*} \rangle^2\right)$$

- Define a SDF:

$$f(\mathbf{p}) = \pm s_{g^*} \sqrt{-2 \log(d(\mathbf{p}))}$$

Surface-alignment regularization

- Regularization using rendered depth map and sampling of visible points:

$$R = \frac{1}{|P|} \sum_{\mathbf{p} \in P} |\hat{f}(\mathbf{p}) - f(\mathbf{p})|$$

- Optional regularization to align normals perpendicular to the surface:

$$R_{\text{normal}} = \frac{1}{|P|} \sum_{\mathbf{p} \in P} \left\| \frac{\nabla f(\mathbf{p})}{\|\nabla f(\mathbf{p})\|_2} - n_{g^*} \right\|_2^2$$

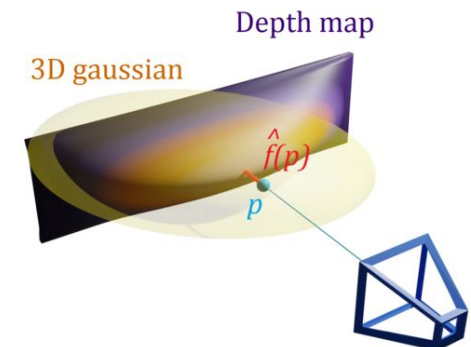


Figure 14: Estimation of the SDF using a rendered depth map. From [1].

[1] Antoine Guédon and Vincent Lepetit. In *Proceedings of the IEEE/CVF Conference on Computer Vision and Pattern Recognition*, pages 5354–5363, 2024.

Surface extraction

- Poisson reconstruction [21]
 - Idea: Estimate an indicator function whose gradient aligns with the surface normals and extract an iso-surface
 - Global and smooth solution
- Sampling points from the level set
 - Unprojected depth as initial guess
 - Local search along viewing ray
 - Using SDF gradients as normal directions

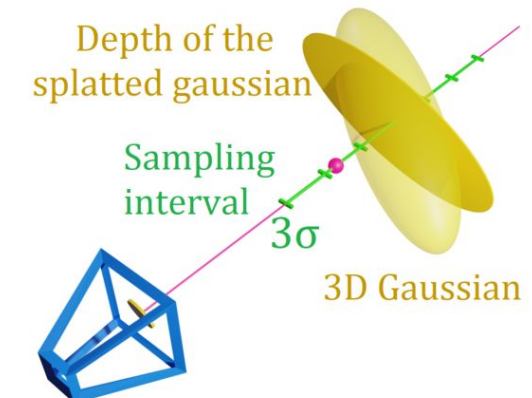


Figure 15: Estimation of the SDF using a rendered depth map. From [1].

[1] Antoine Guédon and Vincent Lepetit. In *Proceedings of the IEEE/CVF Conference on Computer Vision and Pattern Recognition*, pages 5354–5363, 2024.

[21] Michael Kazhdan, Matthew Bolitho, and Hugues Hoppe. Poisson Surface Reconstruction. In *Proceedings of the fourth Eurographics symposium on Geometry processing*, 2006.

Joint refinement

- Optimization using 3DGS with reparametrization
 - Reparametrization of positions using predefined barycentric coordinates and mesh vertex positions
 - Reparametrization of covariance with 1 DoF fixed

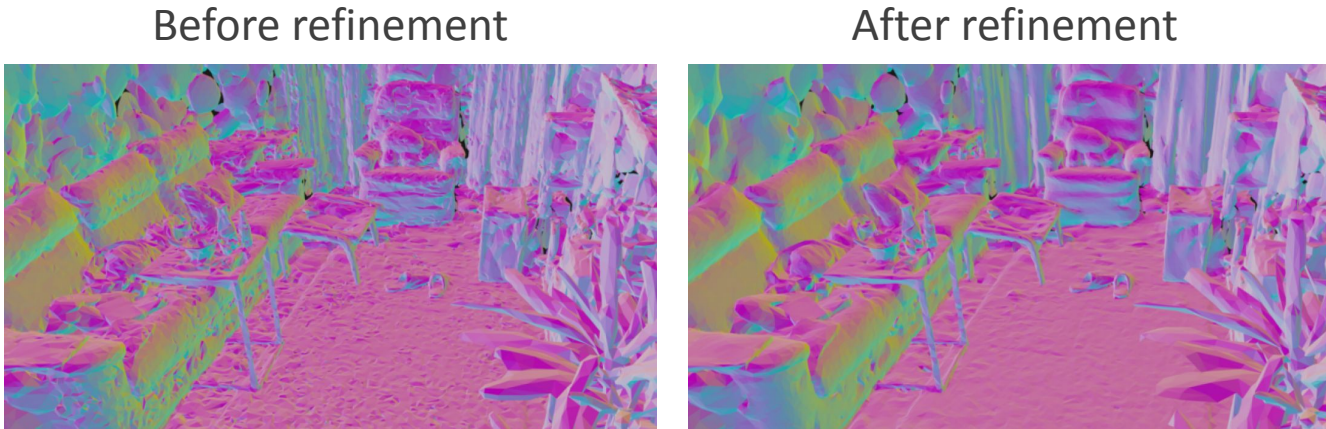


Figure 17: Comparison of the mesh before and after the optional refinement. Adapted from [1].

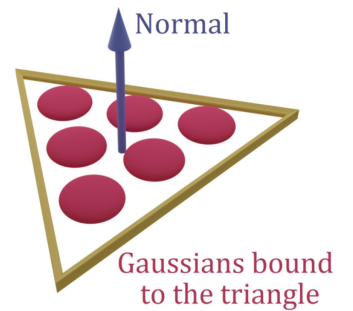


Figure 16: Illustration of Gaussians bound to a mesh triangle. From [1].

[1] Antoine Guédon and Vincent Lepetit. In *Proceedings of the IEEE/CVF Conference on Computer Vision and Pattern Recognition*, pages 5354–5363, 2024.

Contents

1. Introduction
2. Background
3. Methods
- 4. Results**
5. Discussion
6. Conclusion

Surface reconstruction

- Evaluation on DTU [29] dataset using Chamfer distance:

	Scene	24	37	40	55	63	65	69	83	97	105	106	110	114	118	122	Mean	Time
implicit	NeRF [22]	1.90	1.60	1.85	0.58	2.28	1.27	1.47	1.67	2.05	1.07	0.88	2.53	1.06	1.15	0.96	1.49	> 12h
	VolSDF [23]	1.14	1.26	0.81	0.49	1.25	0.70	0.72	1.29	1.18	0.70	0.66	1.08	0.42	0.61	0.55	0.86	> 12h
	NeuS [24]	1.00	1.37	0.93	0.43	1.10	0.65	0.57	1.48	1.09	0.83	0.52	1.20	0.35	0.49	0.54	0.84	> 12h
	Neuralangelo [10]	0.37	0.72	0.35	0.35	0.87	0.54	0.53	1.29	0.97	0.73	0.47	0.74	0.32	0.41	0.43	0.61	> 12h
explicit	3DGS [20]	2.14	1.53	2.08	1.68	3.49	2.21	1.43	2.07	2.22	1.75	1.79	2.55	1.53	1.52	1.50	1.96	11.2m
	SuGaR [1]	1.47	1.33	1.13	0.61	2.25	1.71	1.15	1.63	1.62	1.07	0.79	2.45	0.98	0.88	0.79	1.33	~ 1h
	2DGS [25]	0.48	0.91	0.39	0.39	1.01	0.83	0.81	1.36	1.27	0.76	0.70	1.40	0.40	0.76	0.52	0.80	18.8m
	GOF [26]	0.50	0.82	0.37	0.37	1.12	0.74	0.73	1.18	1.29	0.68	0.77	0.90	0.42	0.66	0.49	0.74	2h
	PGSR [27]	0.34	0.58	0.29	0.29	0.78	0.58	0.54	1.01	0.73	0.51	0.49	0.69	0.31	0.37	0.38	0.53	36m
	GausSurf [28]	0.35	0.55	0.34	0.34	0.77	0.58	0.51	1.10	0.69	0.60	0.43	0.49	0.32	0.40	0.37	0.52	7.2m

Table 1: Quantitative comparison on the DTU dataset. The Chamfer distance and average optimization time are shown. Red, orange, yellow indicate best, second best, third best result, respectively.

- [1] Antoine Guédon and Vincent Lepetit. In *Proceedings of the IEEE/CVF Conference on Computer Vision and Pattern Recognition*, pages 5354–5363, 2024.
[10] Zhaoshuo Li, Thomas Müller, Alex Evans, Russell H Taylor, Mathias Unterath, Ming-Yu Liu, and Chen-Hsuan Lin. Neuralangelo: High-Fidelity Neural Surface Reconstruction. In *Proceedings of the IEEE/CVF Conference on Computer Vision and Pattern Recognition*, pages 8456–8465, 2023.
[20] Bernhard Kerbl, Georgios Kopanas, Thomas Leimkühler, and George Drettakis. 3D Gaussian Splatting for Real-time Radiance Field Rendering. *ACM Trans. Graph.*, 42(4):139–1, 2023.
[22] Ben Mildenhall, Pratul Srinivasan, Matthew Tancik, Jonathan T Barron, Ravi Ramamoorthi, and Ren Ng. NeRF: Representing Scenes as Neural Radiance Fields for View Synthesis. In European Conference on Computer Vision, 2020.
[23] Lior Yariv, Jiajiao Gu, Yoni Kasten, and Yaron Lipman. Volume Rendering of Neural Implicit Surfaces. *Advances in Neural Information Processing Systems*, 34:4805–4815, 2021.
[24] Peng Wang, Lingjie Liu, Yuan Liu, Christian Theobalt, Taku Komura, and Wenping Wang. NeuS: Learning Neural Implicit Surfaces by Volume Rendering for Multi-view Reconstruction. *Advances in Neural Information Processing Systems*, 2021.
[25] Binbin Huang, Zehao Yu, Anpei Chen, Andreas Geiger, and Shenghua Gao. 2D Gaussian Splatting for Geometrically Accurate Radiance Fields. In *SIGGRAPH 2024 Conference Papers*. Association for Computing Machinery, 2024.
[26] Zehao Yu, Torsten Sattler, and Andreas Geiger. Gaussian Opacity Fields: Efficient Adaptive Surface Reconstruction in Unbounded Scenes. *ACM Transactions on Graphics*, 2024.
[27] Danpeng Chen, Hai Li, Weicai Ye, Yifan Wang, Weijian Xie, Shangjin Zhai, Nan Wang, Haomin Liu, Hujun Bao, and Guofeng Zhang. PGSR: Planar-based Gaussian Splatting for Efficient and High-Fidelity Surface Reconstruction. *IEEE Transactions on Visualization and Computer Graphics*, 2024.
[28] Jiepeng Wang, Yuan Liu, Peng Wang, Cheng Lin, Junhui Hou, Xin Li, Taku Komura, and Wenping Wang. GausSurf: Geometry-Guided 3D Gaussian Splatting for Surface Reconstruction. *arXiv preprint arXiv:2411.19454*, 2024.
[29] Rasmus Jensen, Anders Dahl, George Vogiatzis, Engin Tola, and Henrik Aanæs. Large Scale Multi-view Stereopsis Evaluation. In Proceedings of the IEEE conference on computer vision and pattern recognition, pages 406–413, 2014.

Novel view synthesis

- Evaluation on MipNeRF 360 [2] dataset

	Outdoor scenes			Indoor scenes		
	PSNR ↑	SSIM ↑	LPIPS ↓	PSNR ↑	SSIM ↑	LPIPS ↓
NeRF [22]	21.46	0.458	0.515	26.84	0.790	0.370
Instant NGP [30]	22.90	0.566	0.371	29.15	0.880	0.216
MipNeRF360 [2]	24.47	0.691	0.283	31.72	0.917	0.180
3DGS [20]	24.64	0.731	0.234	30.41	0.920	0.189
SuGaR [1]	22.93	0.629	0.356	29.43	0.906	0.225
2DGS [25]	24.34	0.717	0.246	30.40	0.916	0.195
GOF [26]	24.76	0.742	0.225	30.80	0.928	0.167
PGSR [27]	24.45	0.730	0.224	30.41	0.930	0.161
GausSurf [28]	25.09	0.753	0.212	30.05	0.920	0.183

Table 2: Quantitative comparison on the MipNeRF 360 dataset.

[1] Antoine Guédon and Vincent Lepetit. In *Proceedings of the IEEE/CVF Conference on Computer Vision and Pattern Recognition*, pages 5354–5363, 2024.

[2] Ben Barron, Jonathan T and Mildenhall, Dor Verbin, and Peter Srinivasan, Pratul P and Hedman. Mip-NeRF 360: Unbounded Anti-Aliased Neural Radiance Fields. In *Proceedings of the IEEE/CVF conference on computer vision and pattern recognition*, pages 5470–5479, 2022.

[20] Bernhard Kerl, Georgios Kopanas, Thomas Leimkühler, and George Drettakis. 3D Gaussian Splatting for Real-time Radiance Field Rendering. *ACM Trans. Graph.*, 42(4):139–1, 2023.

[22] Ben Mildenhall, Pratul P Srinivasan, Matthew Tancik, Jonathan T Barron, Ravi Ramamoorthi, and Ren Ng. NeRF: Representing Scenes as Neural Radiance Fields for View Synthesis. In European Conference on Computer Vision, 2020.

[25] Binbin Huang, Zehao Yu, Anpei Chen, Andreas Geiger, and Shenghua Gao. 2D Gaussian Splatting for Geometrically Accurate Radiance Fields. In *SIGGRAPH 2024 Conference Papers*. Association for Computing Machinery, 2024.

[26] Zehao Yu, Torsten Sattler, and Andreas Geiger. Gaussian Opacity Fields: Efficient Adaptive Surface Reconstruction in Unbounded Scenes. *ACM Transactions on Graphics*, 2024.

[27] Danpeng Chen, Hai Li, Weicai Ye, Yifan Wang, Weijian Xie, Shangjin Zhai, Nan Wang, Haomin Liu, Hujun Bao, and Guofeng Zhang. PGSR: Planar-based Gaussian Splatting for Efficient and High-Fidelity Surface Reconstruction. *IEEE Transactions on Visualization and Computer Graphics*, 2024.

[28] Jiepeng Wang, Yuan Liu, Peng Wang, Cheng Lin, Junhui Hou, Xin Li, Taku Komura, and Wenping Wang. GausSurf: Geometry-Guided 3D Gaussian Splatting for Surface Reconstruction. *arXiv preprint arXiv:2411.19454*, 2024.

[29] Thomas Müller, Alex Evans, Christoph Schied, and Alexan-der Keller. Instant Neural Graphics Primitives with a Multiresolution Hash Encoding. *ACM Trans. Graph.*, 41(4):1–15, 2022.

Example results

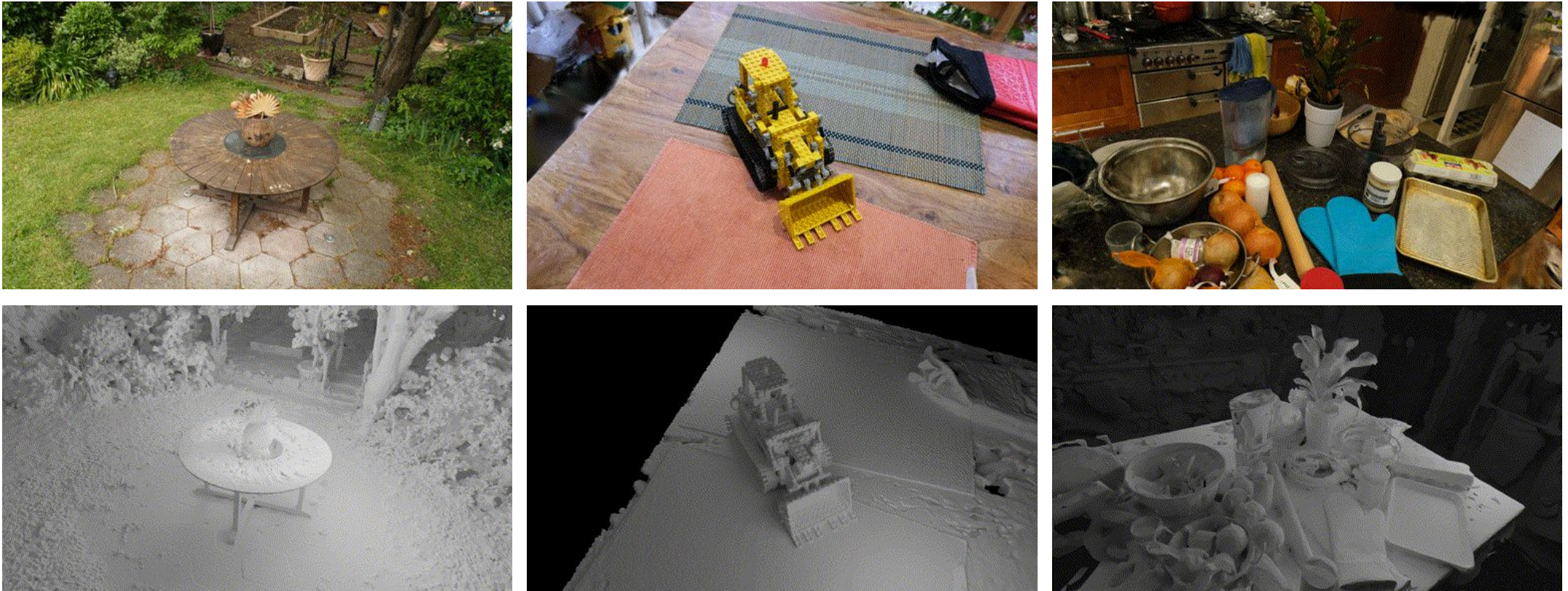


Figure 18: Examples of rendering and reconstructed meshes using SuGaR. From [30]

[30] Antoine Guédon and Vincent Lepetit. <https://github.com/Anttwo/SuGaR>. Accessed: February 25, 2025.

Example applications

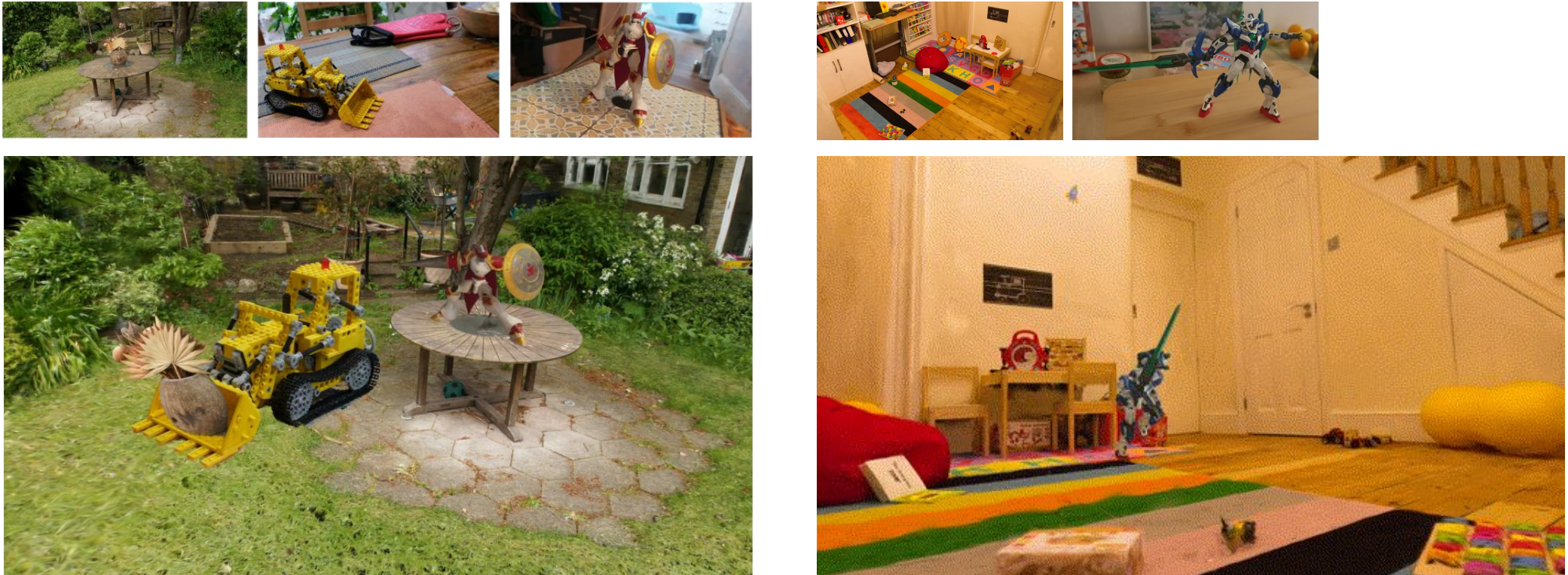


Figure 19: Examples of scene composition and animation using SuGaR. Adapted from [1, 30]

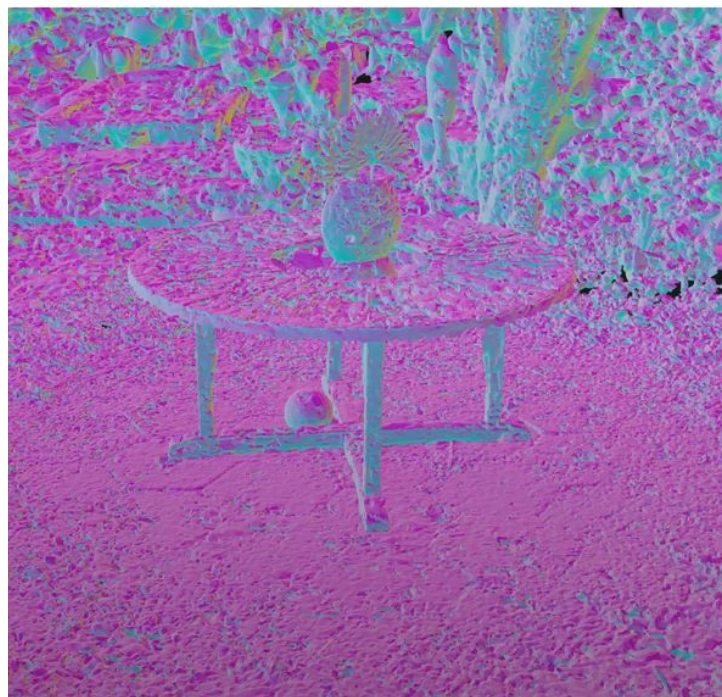
[1] Antoine Guédon and Vincent Lepetit. In *Proceedings of the IEEE/CVF Conference on Computer Vision and Pattern Recognition*, pages 5354–5363, 2024.
[30] Antoine Guédon and Vincent Lepetit. <https://github.com/Anttwo/SuGaR>. Accessed: February 25, 2025.

Comparison with naive approach

No regularization,
Marching Cubes



No regularization,
SuGaR's mesh extraction



SuGaR's regularization,
SuGaR's mesh extraction

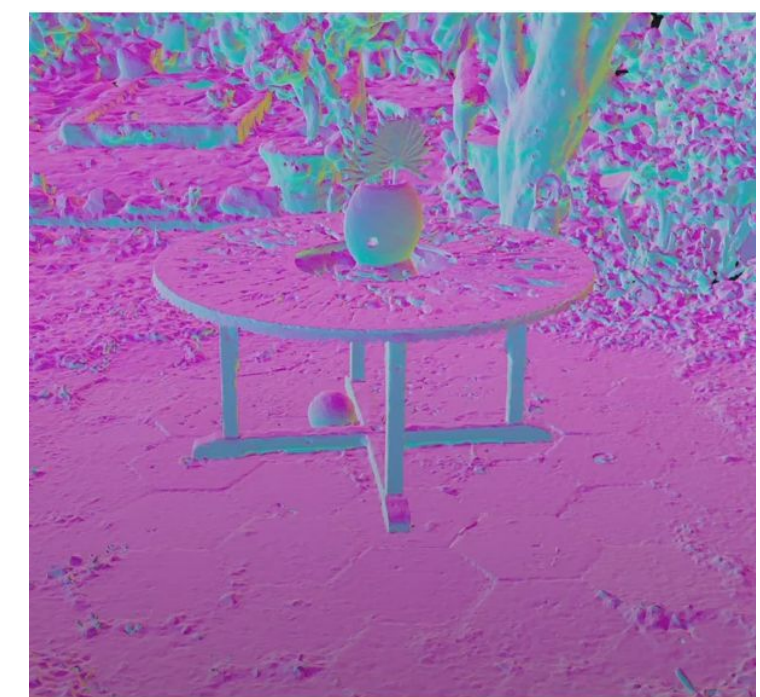


Figure 20: Comparison with reconstructions without SuGaR's regularization and without its mesh extraction method. Adapted from [12].

[12] Antoine Guédon and Vincent Lepetit. Poster for SuGaR. <https://cvpr.thecvf.com/media/PosterPDFs/CVPR%202024/30910.png>. Accessed: February 25, 2025.

Qualitative comparison

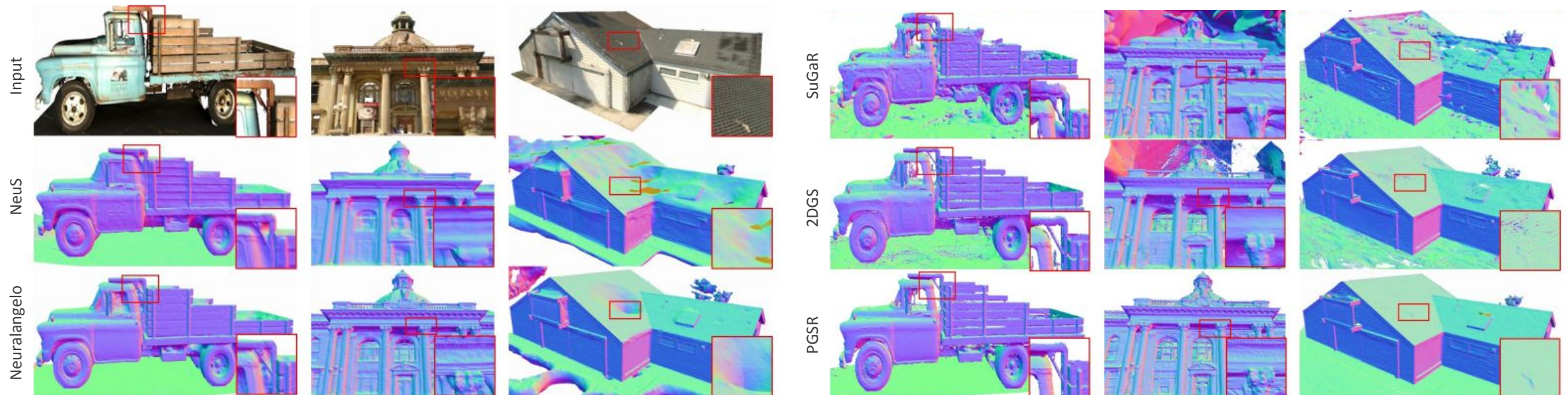


Figure 21: Comparison with concurrent works. Adapted from [31].

[31] Danpeng Chen, Hai Li, Weicai Ye, Yifan Wang, Weijian Xie, Shangjin Zhai, Nan Wang, Haomin Liu, Hujun Bao, and Guofeng Zhang. PGSR: Planar-based Gaussian Splatting for Efficient and High-Fidelity Surface Reconstruction. *IEEE Transactions on Visualization and Computer Graphics*, 2024.

Contents

1. Introduction
2. Background
3. Methods
4. Results
- 5. Discussion**
6. Conclusion

Limitations

- Biased depth estimation
- Poisson reconstruction ignores opacity and scale of Gaussians
- Noisy reconstruction, missing geometry
- Decreased NVS quality
- Manual adjustment of Gaussian parameters for editing
- Lost inductive bias of smoothness from MLP-based NeRF

Further developments

- Collapse flat 3D Gaussians into fully flat 2D Gaussians

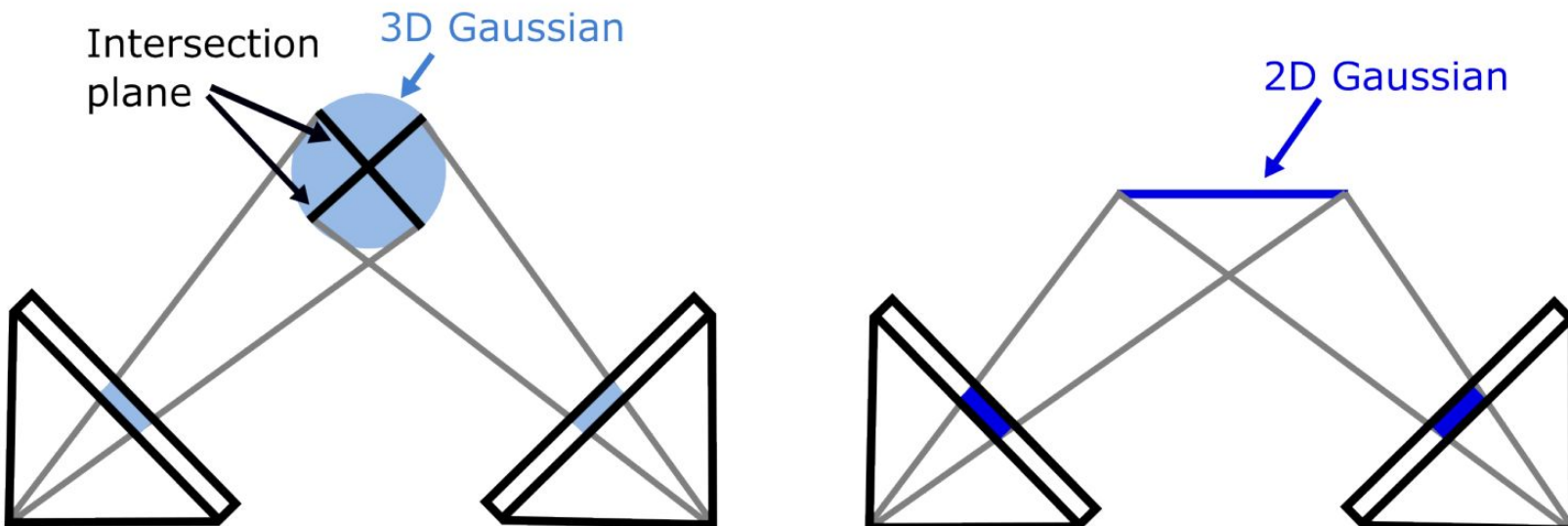


Figure 22: Comparison of 3DGS and 2DGS. 3DGS utilizes different intersection planes for value evaluation when viewing from different viewpoints, resulting in inconsistency. 2DGS provides multi-view consistent value evaluations. From [25].

[25] Binbin Huang, Zehao Yu, Anpei Chen, Andreas Geiger, and Shenghua Gao. 2D Gaussian Splatting for Geometrically Accurate Radiance Fields. In *SIGGRAPH 2024 Conference Papers*. Association for Computing Machinery, 2024.

Contents

1. Introduction
2. Background
3. Methods
4. Results
5. Discussion
- 6. Conclusion**

Conclusion

- Surface reconstruction and high-fidelity real-time rendering
 - Surface-alignment regularization for 3DGS
 - Mesh extraction and refinement
- Decreased appearance modeling capacity
- Hybrid representation for practical applications
- Relies on single-view photometric loss
 - Recent improvements from increased multi-view geometric consistency

References (in order of occurrence)

-
- [1] Antoine Guédon and Vincent Lepetit. SuGaR: Surface-Aligned Gaussian Splatting for Efficient 3D Mesh Reconstruction and High-Quality Mesh Rendering. In *Proceedings of the IEEE/CVF Conference on Computer Vision and Pattern Recognition*, pages 5354–5363, 2024.
 - [2] Ben Barron, Jonathan T and Mildenhall, Dor Verbin, and Peter Srinivasan, Pratul P and Hedman. Mip-NeRF 360: Unbounded Anti-Aliased Neural Radiance Fields. In *Proceedings of the IEEE/CVF conference on computer vision and pattern recognition*, pages 5470–5479, 2022.
 - [3] Zehao Yu, Torsten Sattler, and Andreas Geiger. Gaussian Opacity Fields: Efficient Adaptive Surface Reconstruction in Unbounded Scenes. *ACM Transactions on Graphics*, 2024.
 - [4] Matt Tancik, Ben Mildenhall, Pratul Srinivasan, Jon Barron, and Angjoo Kanazawa. Neural Volumetric Rendering for Computer Vision. *ECCV 2022 Tutorial*, 2022.
 - [5] Prasoon Kumar Vinodkumar, Dogus Karabulut, Egils Avots, Cagri Ozcinar, and Gholamreza Anbarjafari. Deep Learning for 3D Reconstruction, Augmentation, and Registration: A Review Paper. *Entropy*, 26(3):235, 2024.
 - [6] Jeong Joon Park, Peter Florence, Julian Straub, Richard Newcombe, and Steven Lovegrove. DeepSDF: Learning Continuous Signed Distance Functions for Shape Representation. In *Proceedings of the IEEE/CVF conference on computer vision and pattern recognition*, pages 165–174, 2019.
 - [7] Jan-Niklas Dihlmann, Arjun Majumdar, Andreas Engelhardt, Raphael Braun, and Hendrik Lensch. Subsurface Scattering for 3D Gaussian Splatting. *arXiv preprint arXiv:2408.12282*, 2024.
 - [8] William E Lorensen and Harvey E Cline. Marching cubes: A high resolution 3D surface construction algorithm. In *Seminal graphics: pioneering efforts that shaped the field*, pages 347–353. 1998.
 - [9] Ryoshoru. The originally published 15 cube configurations. Wikimedia Commons. <https://commons.wikimedia.org/wiki/File:MarchingCubesEdit.svg>. Accessed: February 17, 2025.
 - [10] Zhaoshuo Li, Thomas Müller, Alex Evans, Russell H Taylor, Mathias Unberath, Ming-Yu Liu, and Chen-Hsuan Lin. Neuralangelo: High-Fidelity Neural Surface Reconstruction. In *Proceedings of the IEEE/CVF Conference on Computer Vision and Pattern Recognition*, pages 8456–8465, 2023.
 - [11] Zhaoshuo Li, Thomas Müller, Alex Evans, Russell H Taylor, Mathias Unberath, Ming-Yu Liu, and Chen-Hsuan Lin. Poster Neuralangelo. <https://research.nvidia.com/labs/dir/neuralangelo/poster.pdf>. Accessed: February 17, 2025.
 - [12] Dylan Ebert. Gaussian Splatting: A New Era for Real-Time 3D Rendering. <https://huggingface.co/blog/gaussian-splatting>. Accessed: February 17, 2025.
 - [13] Shijing Shao, Zhaolong Wang, Zhuang Li, Duotun Wang, Xiangru Lin, Yu Zhang, Mingming Fan, and Zeyu Wang. SplattingAvatar: Realistic Real-Time Human Avatars with Mesh-Embedded Gaussian Splatting. In *Proceedings of the IEEE/CVF Conference on Computer Vision and Pattern Recognition*, pages 1606–1616, 2024.
 - [14] Lining Xu, Vasu Agrawal, William Laney, Tony Garcia, Aayush Bansal, Changil Kim, Samuel Rota Bulò, Lorenzo Porzi, Peter Kortscheder, Aljaž Božič, et al. VR-NeRF: High-Fidelity Virtualized Walkable Spaces. In *SIGGRAPH Asia 2023 Conference Papers*, pages 1–12, 2023.
 - [15] Linfei Pan, Dániel Baráth, Marc Pollefeys, and Johannes L Schönberger. Global structure-from-motion revisited. In *European Conference on Computer Vision*, pages 58–77. Springer, 2024.

References (in order of occurrence)

- [16] Stephen Lombardi. Neural Volumes. <https://stephenlombardi.github.io/projects/neuralvolumes>. Accessed: February 17, 2025.
- [17] Yiheng Xie, Towaki Takikawa, Shunsuke Saito, Or Litany, Shiqin Yan, Numair Khan, Federico Tombari, James Tompkin, Vincent Sitzmann, and Srinath Sridhar. Neural Fields in Visual Computing and Beyond. In *Computer Graphics Forum*, pages 641–676. 2022.
- [18] Florian Pfaff, Gerhard Kurz, and Uwe D Hanebeck. Filtering on the Unit Sphere Using Spherical Harmonics. In *2017 IEEE International Conference on Multisensor Fusion and Integration for Intelligent Systems (MFI)*, pages 124–130. 2017.
- [19] Guikun Chen and Wenguan Wang. A Survey on 3d Gaussian Splatting. *arXiv preprint arXiv:2401.03890*, 2024.
- [20] Bernhard Kerbl, Georgios Kopanas, Thomas Leimkühler, and George Drettakis. 3D Gaussian Splatting for Real-time Radiance Field Rendering. *ACM Trans. Graph.*, 42(4):139–1, 2023.
- [21] Michael Kazhdan, Matthew Bolitho, and Hugues Hoppe. Poisson Surface Reconstruction. In *Proceedings of the fourth Eurographics symposium on Geometry processing*, 2006.
- [22] Ben Mildenhall, Pratul P Srinivasan, Matthew Tancik, Jonathan T Barron, Ravi Ramamoorthi, and Ren Ng. NeRF: Representing Scenes as Neural Radiance Fields for View Synthesis. In *European Conference on Computer Vision*, 2020.
- [23] Lior Yariv, Jiatao Gu, Yoni Kasten, and Yaron Lipman. Volume Rendering of Neural Implicit Surfaces. *Advances in Neural Information Processing Systems*, 34:4805–4815, 2021.
- [24] Peng Wang, Lingjie Liu, Yuan Liu, Christian Theobalt, Taku Komura, and Wenping Wang. NeuS: Learning Neural Implicit Surfaces by Volume Rendering for Multi-view Reconstruction. *Advances in Neural Information Processing Systems*, 2021.
- [25] Binbin Huang, Zehao Yu, Anpei Chen, Andreas Geiger, and Shenghua Gao. 2D Gaussian Splatting for Geometrically Accurate Radiance Fields. In *SIGGRAPH 2024 Conference Papers*. Association for Computing Machinery, 2024.
- [26] Zehao Yu, Torsten Sattler, and Andreas Geiger. Gaussian Opacity Fields: Efficient Adaptive Surface Reconstruction in Unbounded Scenes. *ACM Transactions on Graphics*, 2024.
- [27] Danpeng Chen, Hai Li, Weicai Ye, Yifan Wang, Weijian Xie, Shangjin Zhai, Nan Wang, Haomin Liu, Hujun Bao, and Guofeng Zhang. PGSR: Planar-based Gaussian Splatting for Efficient and High-Fidelity Surface Reconstruction. *IEEE Transactions on Visualization and Computer Graphics*, 2024.
- [28] Jiepeng Wang, Yuan Liu, Peng Wang, Cheng Lin, Junhui Hou, Xin Li, Taku Komura, and Wenping Wang. GausSurf: Geometry-Guided 3D Gaussian Splatting for Surface Reconstruction. *arXiv preprint arXiv:2411.19454*, 2024.
- [29] Thomas Müller, Alex Evans, Christoph Schied, and Alexan-der Keller. Instant Neural Graphics Primitives with a Multiresolution Hash Encoding. *ACM Trans. Graph.*, 41(4):1–15, 2022.
- [30] Antoine Guédon and Vincent Lepetit. <https://github.com/Anttwo/SuGaR>. Accessed: February 25, 2025.
- [31] Danpeng Chen, Hai Li, Weicai Ye, Yifan Wang, Weijian Xie, Shangjin Zhai, Nan Wang, Haomin Liu, Hujun Bao, and Guofeng Zhang. PGSR: Planar-based Gaussian Splatting for Efficient and High-Fidelity Surface Reconstruction. *IEEE Transactions on Visualization and Computer Graphics*, 2024.

Additional slides

Photogrammetry

- Core idea: Stereo vision
- Structure-from-motion (Sfm) reconstructs cameras and points
- Multi-view stereo (MVS) densifies the reconstruction
- Drawback: Long pipeline, susceptible to noise

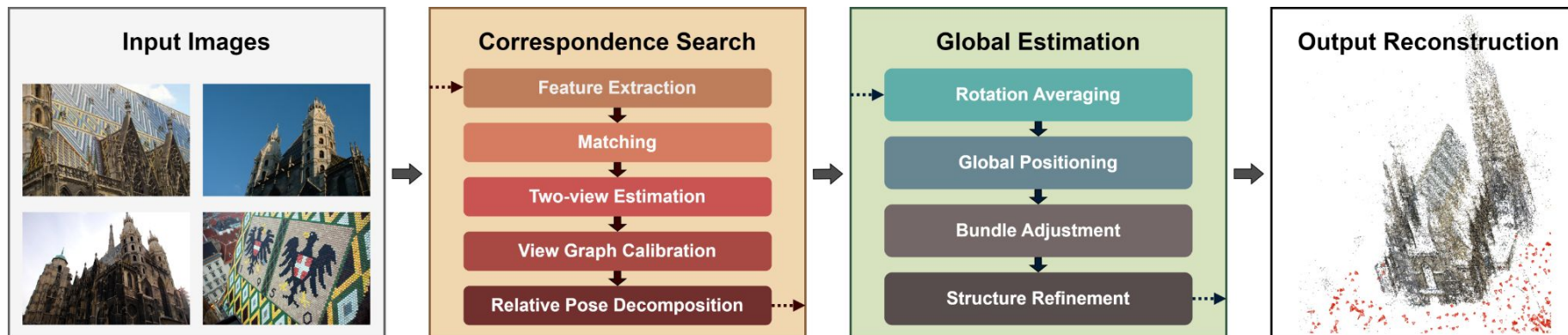


Figure 7: Overview of global SfM method GLOMAP. From [15].

[15] Linfei Pan, Dániel Baráth, Marc Pollefeys, and Johannes L Schönberger. Global structure-from-motion revisited. In *European Conference on Computer Vision*, pages 58–77. Springer, 2024.

The role of meshes

- Standard representation for Computer Graphics
 - Small memory footprint
 - Physics-based simulations (collisions, relighting, etc.)
 - Traditional tools for editing, deforming, rigging, etc.
- Applications for a 3DGS-mesh hybrid
 - Scene editing [1]
 - Virtual humans, animation [13]
 - VR/AR, interactive media [14]
 - and many more...

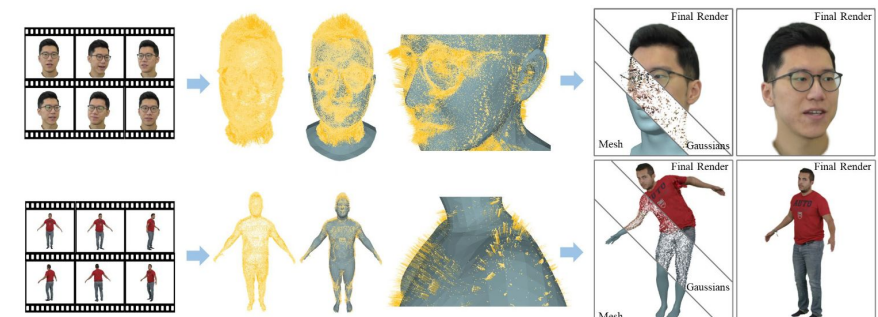


Figure 6: Overview of SplattingAvatar [13]. A trainable embedding technique is employed to associate 3D Gaussians and a mesh, allowing efficient avatar creation and realistic real-time rendering. Adapted from [13].

[13] Shijing Shao, Zhao long Wang, Zhuang Li, Duotun Wang, Xiangru Lin, Yu Zhang, Mingming Fan, and Zeyu Wang. SplattingAvatar: Realistic Real-Time Human Avatars with Mesh-Embedded Gaussian Splatting. In *Proceedings of the IEEE/CVF Conference on Computer Vision and Pattern Recognition*, pages 1606–1616, 2024.

[14] Lining Xu, Vasu Agrawal, William Laney, Tony Garcia, Aayush Bansal, Changil Kim, Samuel Rota Bulò, Lorenzo Porzi, Peter Kortschieder, Aljaž Božič, et al. VR-NeRF: High-Fidelity Virtualized Walkable Spaces. In *SIGGRAPH Asia 2023 Conference Papers*, pages 1–12, 2023.